THE JOURNAL OF PHYSICAL CHEMISTRY C

Article

pubs.acs.org/JPCC

Simultaneous and Sequential Protein and Organothiol Interactions with Gold Nanoparticles

Karthikeshwar Vangala,[†] Kumudu Siriwardana,[‡] Erick S. Vasquez,[‡] Yan, Xin,[§] Charles U. Pittman, Jr.,[†] Keisha B. Walters,[‡] and Dongmao Zhang*[,†]

[†]Department of Chemistry, Mississippi State University, Mississippi State, Mississippi 39762, United States

[‡]Swalm School of Chemical Engineering, Mississippi State University, Mississippi State, Mississippi 39762, United States

[§]National High Magnetic Field Laboratory, Florida State University, Tallahassee, Florida 32310-3706, United States

Supporting Information

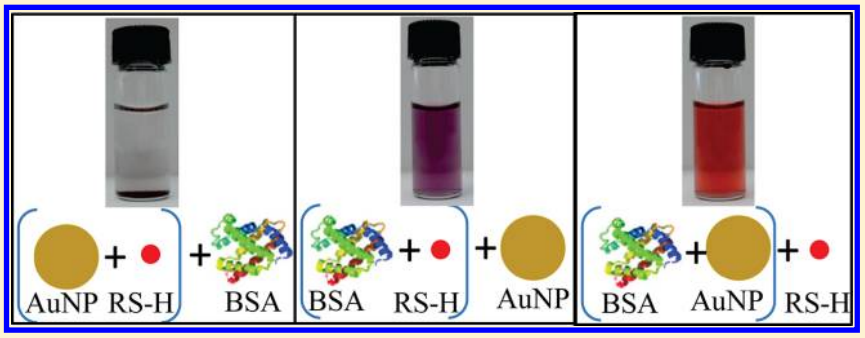

ABSTRACT: Proteins and organothiols (OTs) are known to have high affinity for gold nanoparticles (AuNPs). Systematic investigation of protein and OT coadsorption onto AuNPs is, however, mostly an unexplored area. Presented here is a comparison of simultaneous and sequential protein and OT interactions with AuNPs in which a protein and an OT are either simultaneously or sequentially added to colloidal AuNPs. Using bovine serum albumin (BSA) as the model protein and eight model organothiols, both the protein and the OT were coadsorbed onto AuNPs in samples formed by sequential or simultaneous addition. AuNP stability against OT-adsorption-induced AuNP aggregation differed significantly among the AuNP/OT and AuNP/BSA/OT mixtures. The stability of AuNPs in the AuNP/BSA/OT mixtures with the same compositions increased from (AuNP/OT)/BSA to AuNP/(BSA/OT) and finally (AuNP/BSA)/OT (where the two components inside the parentheses are mixed first followed by the addition of the third component). Aging the (AuNP/BSA) mixtures before OT addition also increased the AuNP stability in (AuNP/BSA)/OT samples. This sequence and aging dependence of AuNP stability indicates that protein and OT coadsorption onto AuNPs is kinetically controlled. It also offers a plausible explanation to the large discrepancy in the binding constants reported for the BSA interaction with AuNPs (from 10^5 to 10^{11} M^{-1}). The work is important for AuNP biological/biomedical applications because AuNPs encounter a mixture of proteins and OTs in addition to other molecular species in biofluids.

INTRODUCTION

Understanding molecular-level ligand interfacial interactions with gold nanoparticles (AuNPs) is critically important for many AuNP applications in biosensing, drug delivery, catalysis, etc.[1,2] Proteins and organothiols (OT) are known to have high binding affinities to gold nanoparticles,[3,4] and they are used extensively for AuNP surface modifications to improve functionality, stability, target specificity, or to reduce the AuNP toxicity in biological/biomedical applications.[1,2] OT binding to AuNPs is widely accepted to occur through the formation of covalent Au−S bonds,[3] but the exact mechanism of protein interaction with AuNPs is much less understood. For example, binding constants from ~10^5 to 10^{11} M^{-1} has been reported for BSA binding with AuNPs,[5−8] one of the most extensively studied protein/AuNP binding models. Proteins are biomacromolecules with diverse structures and functions. Therefore, the binding of proteins with AuNPs most likely involves multiple intermolecular forces including covalent binding, electrostatic, hydrophobic, and van der Waals interactions.[9−12] Some researchers attribute BSA interactions with citrate-reduced AuNPs mainly to electrostatic interactions between positively charged lysine groups and the negatively charged citrate-coated AuNPs[9,10] Others suggest the binding occurs through covalent interactions of cysteine sulfur groups and the AuNP surface.[6,11]

We have recently studied OT interactions with BSA-stabilized AuNPs to enhance understanding of protein/AuNP interactions.[13] The protein coating layer was found to be highly

Received: October 11, 2012
Revised: December 28, 2012
Published: December 28, 2012

ACS Publications © 2012 American Chemical Society

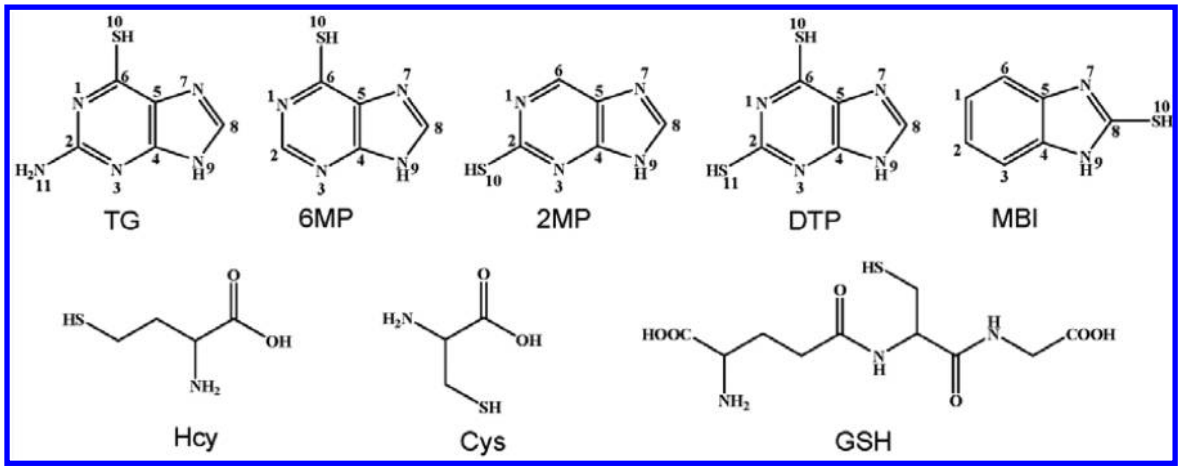

Figure 1. Chemical structures of 6-thioguanine (TG), 6-mercaptopurine (6MP), 2-mercaptopurine (2MP), dithiopurine (DTP), mercaptobenzimidazole (MBI), homocysteine (Hcy), cysteine (Cys), and glutathione (GSH).

porous and permeable. Small molecules such as mercaptobenzimidazole (MBI), cysteine (Cys), homocysteine (Hcy), and glutathione (GSH) were shown to diffuse through the protein coating layer and self-assemble onto AuNPs.[13] Importantly, the subsequent OT adsorption onto the protein-coated AuNPs does not induce any significant BSA desorption even after 3 days of sample incubation.[13] This result implies that the BSA binding affinity with AuNPs is at least comparable to that of AuNP/OT binding, suggesting BSA cysteine residues are binding with AuNPs. Otherwise, one would expect OT should readily displace BSA from the AuNPs if the BSA and AuNP binding involves only nonspecific electrostatic interactions. In contrast, the displacement of Au−S covalently bound ligands on AuNPs is an extremely slow process and often requires elevated temperatures.[14,15]

Herein we report the simultaneous and sequential protein and OT binding to AuNPs. The protein BSA and an OT were added simultaneously or sequentially into the colloidal AuNP solution. A key focus of this study explored how the sample preparation sequence affects the properties of the AuNP/BSA/OT samples. Addressing this question enriches our knowledge of multicomponent ligand interactions with AuNPs, which has many practical applications. In realistic biological/biomedical applications, AuNPs encounter a complex mixture including proteins and OTs, not OTs or proteins alone.[16] Thus, knowledge of the structure and properties of AuNPs in protein/OT mixtures can be critical for designing biocompatible AuNPs for biological/biomedical applications.

The inclusion of different OTs allows evaluation of how OT structure affects their competitive binding to AuNPs versus BSA. In this study four thiopurine derivatives were used as our model OTs in addition to MBI, Cys, Hcy, and GSH, the OTs that we used for studying the sequential OT and BSA interactions with AuNPs.[13] The selected thiopurines included thioguanine (TG), 6-mercaptopurine (6MP), 2-mercaptopurine (2MP), and dithiopurine (DTP). They differ in the position and the number of thiol or amino functional groups, both known to have high binding affinity to AuNPs (Figure 1). The samples used in this work were denoted as (AuNP/OT)/BSA, AuNP/(BSA/OT), and (AuNP/BSA)/OT where the components in the inner parentheses were added first followed by the third component.

EXPERIMENTAL SECTION

Materials and Equipment. All the chemicals used were purchased from Sigma-Aldrich. BSA with a purity of 97% (lot # 064 K1251) was used as received. Nanopure water (ThermoScientific) was used in all measurements. The catalog numbers and purities of the sample are shown in the Supporting Information (Table S1). The stock solutions of the thiopurine derivatives were freshly prepared as prolonged storage (more than 1 day) induces change in the UV−vis absorbance of these solutions, indicating sample degradation. Time-resolved UV−vis spectra were acquired using an Olis HP 8452 diode array spectrophotometer.

AuNP Synthesis. AuNPs were synthesized using the citrate reduction method as described previously.[13] Gold(III) chloride trihydrate (0.0415 g, 0.105 mmol) was dissolved in 100 mL of distilled water and refluxed with vigorous stirring. Then, 10 mL of aqueous 1.14% (w/v) sodium citrate dihydrate was added to the solution after reflux was reached, and refluxing was continued for 20 min. The average AuNP size was ∼13 nm in diameter (Figure S1). The concentration of AuNPs was calculated as 11.1 nM by assuming that all gold(III) ions were reduced to gold(0). This was consistent with the AuNP concentration estimated using the UV−vis absorbance of the as-synthesized AuNPs.[17]

Time-Resolved UV−vis Spectroscopy. The time-resolved UV−vis spectra of AuNP/(BSA/OT), (AuNP/BSA)/OT, and (AuNP/OT)/BSA samples were acquired immediately after the addition of the final component into the solution. The spectral acquisition of AuNP/(BSA/OT) was continued for a period of 15 h with a time delay of 10 min between each acquisition. The time-resolved UV−vis spectra for the (AuNP/BSA)/OT and (AuNP/OT)/BSA samples were acquired at different time intervals for a period of 3 days. The integration time for each time-resolved UV−vis was 2 s.

Surface-Enhanced Raman Spectroscopy (SERS). SERS spectra were acquired after depositing a 10 μL of aggregated sample of AuNP/OT on a Ramchip slide. A Ramchip slide is a normal Raman substrate that has essentially no fluorescence or Raman background.[18] The AuNP/DTP sample was aggregated by adding 20% KCl. SERS spectra were acquired after focusing the laser onto the settled AuNP aggregate using a 10× objective. An integration time of 20 s and a 1.3 mW HeNe laser (632 nm) were used for all the samples.

dx.doi.org/10.1021/jp310085u | J. Phys. Chem. C 2013, 117, 1366−1374

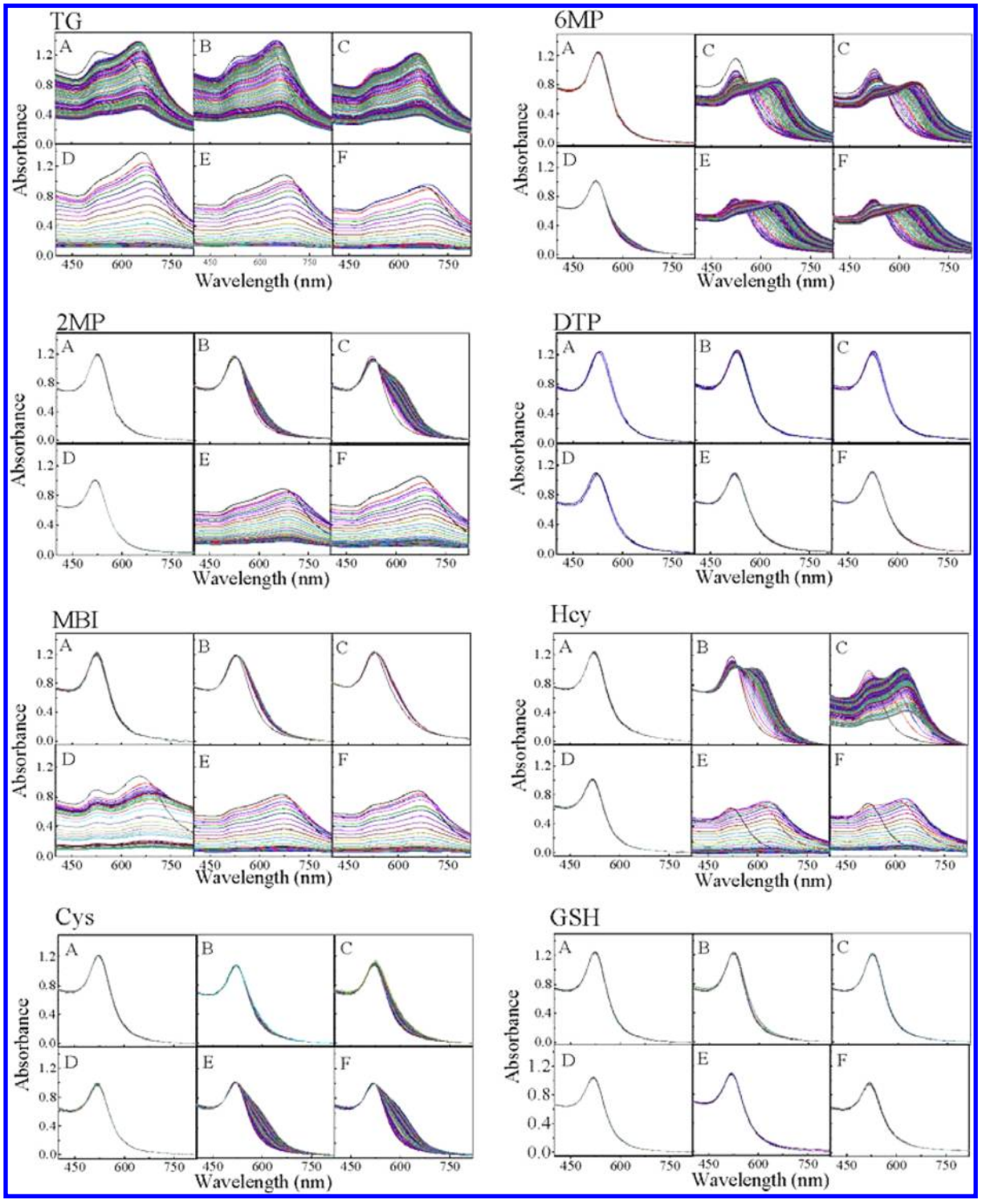

Figure 2. Time-resolved UV−vis spectra of (A−C) AuNP/(BSA/OT) samples and (D−F) are for AuNP/OT in which no BSA is used. The OT concentration is (A, D) 3.3 μM, (B, E) 16.6 μM, and (C, F) 30 μM, respectively. The concentrations of AuNPs and BSA were 3.7 nM and 3.3 μM, respectively.

AuNP/(BSA/OT) and AuNP/OT Sample Flocculation Studies. A 500 μL BSA/OT mixture was added to 250 μL of AuNP colloidal solution followed by incubation for 2 min. A 250 μL 20% KCl aqueous solution was then added to initiate the flocculation. The UV−vis spectrum was acquired immediately after the KCl addition. Similar experiments were done for AuNP/OT mixtures with no BSA which served as control samples. The nominal AuNP, BSA, and OT concentrations in these samples were 3.7 nM, 2.5 μM, and 12.5 μM, respectively.

Dynamic Light Scattering (DLS), Electrophoresis Light Scattering (ELS), and Phase Angle Light Scattering (PALS). Light scattering measurements were collected at 25 °C using a ZetaPALS analyzer with a laser wavelength of 659 nm (Brookhaven Instruments Corporation (BIC), Holtsville, NY). Particle size and PALS measurements were detected at a 90°

dx.doi.org/10.1021/jp310085u | J. Phys. Chem. C 2013, 117, 1366−1374

angle and ELS data with the detector at 15°. The samples were allowed to stabilize in the cuvette for 3 min prior to data collection. A total of 10 measurements (2 min per measurement) were carried out on each sample for particle size determination using the mean number diameter. BIC Particle Solutions software v2.0 was utilized for data collection and analysis.

RESULTS AND DISCUSSION

Simultaneous BSA and OT Interactions with AuNPs (AuNP/(BSA/OT)). The AuNP stability against aggregation induced by ligand adsorption in the AuNP/OT and AuNP/(BSA/OT) samples was monitored using time-resolved UV−vis measurements. Previous research established that AuNP localized surface plasmonic resonance (LSPR) absorbance is sensitive to both AuNP ligand binding and AuNP aggregation.[4,9,19−22] The spectral change in AuNP LSPR features induced by AuNP aggregation is much more pronounced compared to that induced by ligand adsorption that usually shifts the peak LSPR wavelength by several nanometers. AuNP aggregation can red-shift the AuNP peak UV−vis wavelength by tens of nanometers.

When the freshly synthesized AuNPs are mixed with BSA alone, the AuNPs' LSPR peak is immediately shifted from 519 to 524 nm. The AuNPs in the AuNP/BSA mixture remain stable (no aggregation) during the entire 3 day experimental period (Figure S2). This observation is consistent with our recent report,[13] and it indicates that BSA has bonded to AuNPs. However, when mixed with OTs or BSA/OT mixtures, AuNPs exhibit a wide stability range against the OT-adsorption induced aggregation. Figure 2 shows the time-resolved UV−vis spectra obtained with all the AuNP/OT and AuNP/(BSA/OT) samples. AuNP aggregation in some of the samples was evident by the immediate increase in the AuNP UV−vis absorbance at wavelengths larger than 650 nm. Extensive aggregation led to AuNP settling to the bottom of the UV−vis cuvette, as evident by the total disappearance of the AuNP LSPR features. Figure 3 shows plots of the UV−vis absorbance at 650 nm versus time. These plots were extracted from the time-resolved UV−vis spectra in Figure 2. For the sake of clarity, Figure 3 only showed the UV−vis time courses for the AuNP/OT and AuNP/(BSA/OT) samples in which AuNPs aggregated upon the ligand adsorption.

The two most important parameters in the samples used in Figure 2 are the OT and BSA concentrations. The amount of the BSA added onto the AuNPs exceeded the full monolayer BSA binding capacity for these AuNPs, assuming the footprint of each BSA molecule on the AuNP surface to be 25 nm^2.[13] The 3.3, 16.6, and 30 μM OT concentrations in the AuNP solutions correspond to 0.4, 2.1, and 3.7 times of the full monolayer packing capacity of the AuNPs, which was estimated by assuming that each of the OTs has a similar footprint to MBI on AuNP (574 pmol/cm^2).[23] The inclusion of different amounts of these OTs allows exploration of how OT concentration affects the competitive BSA and OT binding with AuNPs.

The stability of AuNPs against aggregation when OTs are adsorbed depends critically on the OT molecular structures and concentrations. The AuNP/OT and AuNP/(BSA/OT) solutions are stable when the OT is present below the full monolayer packing capacity for 6MP, 2MP, Hcy, and Cys. However, when the OT concentration exceeds full monolayer capacity, the AuNPs in these samples exhibited a different

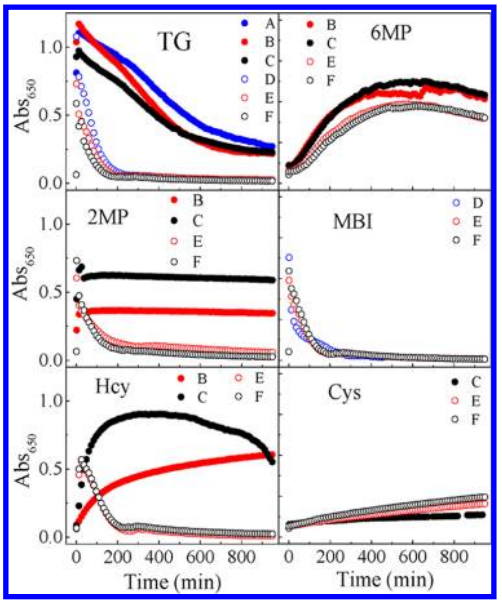

Figure 3. UV−vis absorbance at 650 nm versus time for aggregated (filled circles) AuNP/(BSA/OT) and aggregated (open circles) AuNP/OT samples. The OT concentrations were 3.3 μM (blue), 16.6 μM (red), and 30 μM (black). The legends show the OT samples in Figure 2 to which the time courses correspond. The concentrations of AuNPs and BSA were 3.7 nM and 3.3 μM, respectively.

degree of aggregation. OT interactions with AuNPs have been a topic of intensive research.[3,24] However, few have studied the OT concentration dependence of the AuNP stability with the ligand adsorbed.[25,26] In addition, cross-comparisons of the aggregation characteristics of AuNPs with bound OTs for relatively large numbers of different OTs have, to our knowledge, not been reported.

The OT adsorption onto AuNPs was experimentally confirmed for all the AuNP/OT mixtures: The OT adsorption can be inferred in the AuNP/OT samples by the AuNP aggregation upon OT addition. AuNPs in DTP and GSH containing solutions are entirely stable regardless of the OT concentrations. Nevertheless, the OT adsorption in these solutions can be deduced from the increase in the AuNP LSPR peak absorption wavelength when AuNPs are mixed with DTP or GSH (Figure S2). Similarly, the interactions of 6MP, 2MP, Hcy, and Cys at submonolayer concentrations on the AuNPs are also inferred from the increase of the LSPR peak absorption of the AuNPs upon the addition of OTs (Figure S3). In addition, the OT adsorption onto AuNPs can also be confirmed with SERS measurements (Figures S4 and S5).

SERS is among the few analytical methods that may be capable of detecting ligand structure on AuNPs. Our recent SERS measurement shows that in pH > 2 solutions, MBI is adsorbed as a thiolate form on the AuNPs.[27] Given the high structural similarity between MBI and the thiopurine derivatives, we believe that thiopurine derivatives were also adsorbed as thiolate on the AuNPs under our experimental conditions (pH ∼7). The formation of covalent Au-sulfur binding between the amino acid thiols (Hcy, Cys, and GSH) and AuNPs was experimentally confirmed via their respective SERS spectra that showed that the S−H stretch Raman feature spectra is completely absent in their SERS spectra (Figure S5).

TG and MBI are the most effective of all the OTs at inducing AuNP aggregation and settling. Complete AuNP aggregation and settlement were observed even when only submonolayer

dx.doi.org/10.1021/jp310085u | J. Phys. Chem. C 2013, 117, 1366−1374

concentrations of MBI and TG were added into the AuNP/OT solutions. The AuNPs in the AuNP/Hcy and AuNP/2MP samples are stable as colloidal solutions at submonolayer OT concentrations, but when mixed with excess ligand concentrations they aggregated and eventually settled (plots III and VI in Figure 3). The stability of the AuNPs which had adsorbed Cys is somewhere between those of AuNPs with GSH and Hcy. AuNPs with submonolayer concentrations of Cys are stable in solution, but a degree of AuNP aggregation appears if excess Cys is present in solution. However, the extent of the AuNP aggregation is so subtle that it is elusive to decipher by visual examination as the solution remains pinkish after storing for 3 days (Figure S6). This may explain why some previous reports stated that AuNPs are stable in Cys-containing solutions.[28,29]

Despite their structural similarities, the thiopurine derivatives differ significantly in their ability to induce AuNP aggregation. While submonolayer TG concentrations induce immediate AuNP aggregation, AuNP/DTP samples are stable even when the DTP concentrations are 3 times higher than the full AuNP monolayer packing capacity. The stabilities of the 6MP- and 2MP-coated AuNPs are somewhere between those of TG and DTP. Submonolayer 2MP- and 6MP-coated AuNPs were mostly stable in solution, but excess 2MP and 6MP both cause AuNPs to aggregate. Additionally, AuNP settling occurs in the 2MP/AuNP sample. The ability of these thiopurine derivatives to induce AuNP aggregation and settlement follows the order TG > 2MP > 6MP > DTP.

Attempts to probe the specific mechanism responsible for the differences in the AuNP aggregation among thiopurine-functionalized AuNPs were not successful. Ligand-coated AuNP stability should relate to the ligand structure, composition, and surface packing densities on the AuNP surfaces as well as all the possible interparticle interactions among OT-functionalized AuNPs. Unfortunately, determination of these parameters has not yet been possible. Each of the thiopurine derivatives tested can exist as multiple tautomeric/ionic forms in solution and when adsorbed to AuNPs. For example, neutral DTP in solution alone has over 10 possible tautomeric forms.[30] Thiopurines can bind monodentately as their thione, thiol, and/or thiolate forms when adsorbed to the AuNP surfaces. Bidentate or multivalent binding is also possible where both nitrogen and sulfur atoms are in direct contact with AuNP surfaces. This further complicates the determination of the thiopurine structures and compositions on the AuNPs. Nevertheless, the drastically different AuNP stabilities among the thiopurine derivative solutions indicate the aggregation is very sensitive to small structural modification in the surface-bound ligand structures. This conclusion is also consistent with the significant difference in the AuNP stability between the Cys and Hcy samples.

Several results indicated OT and BSA coadsorption occurred in all the AuNP/(BSA/OT) samples. OT and BSA coadsorption onto AuNPs was obvious for TG, 6MP, 2MP, MBI, Hcy, and Cys containing samples because the degree of or rate of aggregation differed markedly for AuNP/(BSA/OT) when AuNPs were mixed with BSA or with OT alone. BSA adsorption in the AuNP/(BSA/DTP) and AuNP/(BSA/GSH) samples was experimentally confirmed by flocculation studies. This showed the presence of BSA further enhances the AuNP stability against electrolyte (KCl) induced aggregations (Figure 4). DTP or GSH adsorption onto the gold in their respective AuNP/(BSA/OT) samples was deduced from quantitative MBI adsorption experiments. The amount of MBI adsorbed is

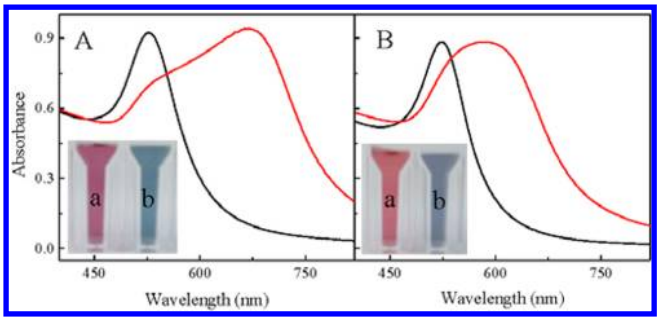

Figure 4. UV−vis spectra of (black) (AuNP/(BSA/OT))/KCl and (red) (AuNP/OT)/KCl samples. Inset: photographs of (a) (AuNP/(BSA/OT))/KCl and (b) (AuNP/OT)/KCl solutions taken 1 min after addition of 250 μL OF KCl to the 750 μL OF AuNP/(BSA/OT) or AuNP/OT solutions. The OTs used in plots A and B were DTP and GSH, respectively. The concentrations of AuNPs, BSA, and OT in the samples before KCl additions were 3.7 nM, 3.3 μM, and 16.6 μM, respectively. The initial concentration of KCl was 20% (w/v).

significantly smaller in the (AuNP/(BSA/DTP))/MBI and (AuNP/(BSA/GSH))/MBI samples than that in the (AuNP/BSA)/MBI samples (Table S2). Thus, both DTP and GSH are bound to some of the surface when BSA is present, subsequently limiting how much MBI can bind later. This OT coadsorption with BSA onto AuNPs is not surprising based on the recent experimental observation of OT adsorption onto AuNPs, even when the OT is added after BSA has been mixed with AuNPs.[13]

BSA's ability to stabilize AuNPs against aggregation due to OT adsorption is drastically different for different OTs. This is revealed by comparing the time-resolved UV−vis spectra of AuNP/(BSA/OT) samples with their respective AuNP/OT controls (Figure 2). Among all the OTs tested, BSA is most effective in preventing MBI and 2MP from causing AuNP aggregation and settlement. In other words, BSA is the dominant ligand determining the AuNP aggregation characteristics in the simultaneous BSA/OT exposure in AuNP/(BSA/MBI) and AuNP/(BSA/2MP) samples. For TG, 6MP, Cys, and Hcy, the presence of BSA only reduces the rate and extent of the AuNP aggregation (Figures 2 and 3) but does not prevent this aggregation. These OTs are the dominant ligands in determining AuNP aggregation characteristics of their corresponding AuNP/(BSA/OT) samples. Nanoparticle stability in the AuNP/(BSA/DTP) and AuNP/(BSA/GSH) samples is expected because AuNPs are stable when mixed with BSA, GSH, or DTP alone.

Presumably the AuNP/(BSA/OT) sample stabilities, for which OT adsorption alone (without BSA) induces AuNP aggregation, should depend on the BSA and OT architectures on AuNP surfaces. There are three possible architecture classes that may be present simultaneously on the same AuNP for coadsorbed BSA and OT (Figure 5). First, the protein and OT on the AuNPs could be directly linked to AuNPs through the formation of covalent sulfur−Au bonds. Second, protein adsorbs onto the OT overlayer on the AuNP surface. Finally, OT can adsorb onto the BSA overlayer on AuNPs. While BSA and OT direct bonding to AuNPs is expected for all the AuNP/(BSA/OT) samples, the existence of the secondary BSA or OT adsorption in the AuNP/(BSA/OT) samples; i.e., the ligand adsorption through association with either a OT or a BSA overlayer on AuNPs will depend critically on OT structure.

dx.doi.org/10.1021/jp310085u | J. Phys. Chem. C 2013, 117, 1366−1374

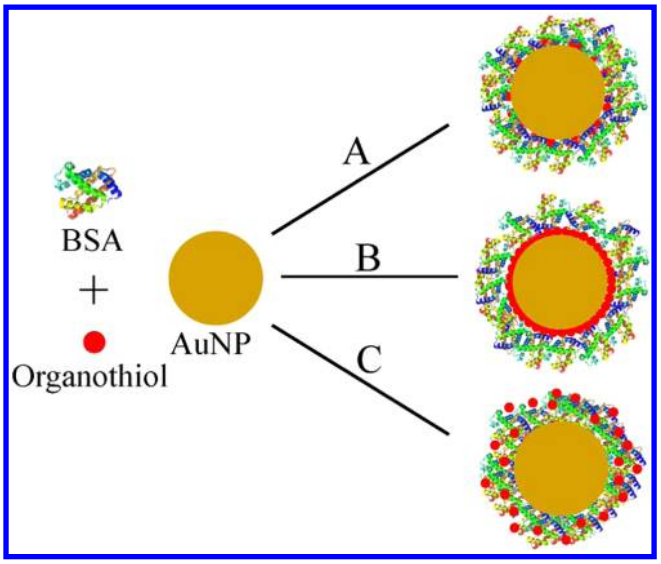

Figure 5. Schematic representation of the three possible architectures of BSA and OT coadsorption onto AuNPs. (A) Both BSA and OT are directly adsorbed onto AuNPs. (B) OT is directly adsorbed on AuNPs, but BSA is adsorbed through the bound OT overlayer. (C) BSA is directly adsorbed on AuNPs, but OT molecules are adsorbed through the BSA.

Sequential OT and BSA Interactions with AuNPs ((AuNP/OT)/BSA). The possible secondary BSA adsorption onto AuNPs after OT had already been adsorbed was probed by examining the stability of (AuNP/OT)/BSA samples in which BSA was added 10 s after first mixing AuNPs with excess OTs (Figure 6). Our presumption is that when substantial secondary BSA adsorption occurs, the AuNP stability in the (AuNP/OT)/BSA samples should resemble that in AuNP/BSA. Otherwise, (AuNP/OT)/BSA samples should aggregate similarly to AuNP/OT. The delay time between BSA and OT mixing was determined by two considerations. On one hand, the delay time should be long enough so that most OT adsorption is completed before BSA addition to eliminate the direct BSA adsorption onto AuNPs. On the other hand, the delay time should be short enough to prevent excessive AuNP aggregation induced by OT adsorption. Otherwise, the aggregated AuNP will settle to the bottom of the cuvette regardless of the status of BSA adsorption. Our recent work[13] on MBI adsorption onto AuNP showed that OT adsorption is an exceedingly rapid process. Over 90% of MBI adsorption occurs within the first 2 s of mixing 16.6 μM MBI with AuNPs.[13] The 10 s delay time applied between the OT and BSA addition should be sufficient to ensure complete OT adsorption (>95% for example) onto AuNPs before the addition of the BSA.

Time-resolved UV–vis spectra (Figure 6) showed that the subsequent BSA addition has no significant effect on the AuNP aggregation for AuNP/TG, AuNP/6MP, and AuNP/Hcy samples. However, delayed BSA addition almost entirely stopped AuNP aggregation induced by OT adsorption in the initial AuNP/MBI and AuNP/2MP samples. This result unambiguously indicates the BSA binding occurs with MBI- and 2MP-coated AuNP because without the subsequent BSA addition, the MBI or 2MP would cause complete AuNP aggregation and settlement (Figure 2). Since AuNP surfaces are likely densely packed with MBI and 2MP before the BSA addition, the only sensible explanation is that secondary BSA

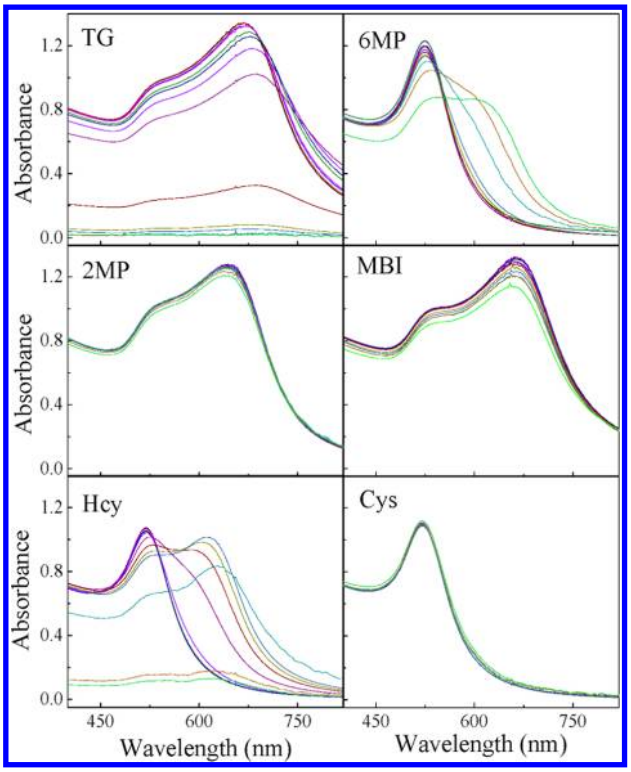

Figure 6. Representative time-resolved UV–vis spectra of several (AuNP/OT)/BSA solutions where BSA was added 10 s after OT addition to AuNPs. The spectra shown in each panel were taken at 7 s, 30 s, 1 min, 10 min, 2 h, 12 h, 1 day, and 3 days after the addition of BSA. The concentrations of AuNP, OT, and BSA used in all six systems were 3.7 nM, 16.6 μM, and 3.3 μM, respectively.

adsorption possibly occurs in (AuNP/MBI)/BSA and (AuNP/2MP)/BSA solutions; i.e., the BSA adsorbs onto the MBI or 2MP overlayer. BSA displacement of preadsorbed MBI or 2MP is excluded because it is known that displacing OTs from AuNPs is an extremely slow process, often requiring elevated temperature.[14,15]

Regardless of whether MBI binds to AuNPs as a thione or thiolate, the distal end of absorbed MBI is a phenyl ring.[23] Assuming all OTs are also adsorbed onto AuNPs through Au–S bonds, the distal ends of the adsorbed TG, 6MP, 2MP, and DTP have amino groups and are more hydrophilic than the distal end phenyl group of adsorbed MBI. Thus, BSA adsorption onto the MBI-covered AuNPs should be easier than to AuNPs covered with other more hydrophilic OTs, as it is known that BSA has high binding affinity to Au surfaces functionalized with hydrophobic molecules.[31,32] However, the exact reason why BSA can also stop the aggregation of AuNPs coated with 2MP, but not when coated with TG and 6MP, is currently unclear.

The AuNP aggregation behavior of the AuNP/(BSA/MBI) and AuNP/(BSA/2MP) in Figure 2 is similar to their corresponding (AuNP/MBI)/BSA and (AuNP/2MP)/BSA samples in Figure 6. This strongly suggests that secondary BSA adsorption is the reason for the high AuNP stability in the AuNP/(BSA/MBI) and AuNP/(BSA/2MP) samples. Otherwise, extensive AuNP aggregation would occur in the simultaneous addition samples where MBI and 2MP were ~5 and ~10 times more concentrated than BSA. In these samples the OT likely dominates the immediate AuNP surface coating layer because of its high concentration and small molecular size.

dx.doi.org/10.1021/jp310085u | J. Phys. Chem. C 2013, 117, 1366–1374

Both effects can lead to a faster AuNP binding kinetics for OTs than that for the large BSA molecules.

Dynamic Light Scattering and ξ-Potential Measurements. Important insights can be derived from the DLS measurements conducted with DTP, GSH, and Cys (Table 1),

Table 1. DLS Particle Size in Diameter (nm)[a]

samples	organothiols		
	DTP	GSH	Cys
AuNP/OT	13.8 ± 1.3	13.5 ± 1.4	13.3 ± 1.4
AuNP/BSA	19.9 ± 1.4	19.9 ± 1.4	19.9 ± 1.4
(AuNP/BSA)/OT	19.8 ± 1.8	20.1 ± 1.8	19.4 ± 1.7
AuNP(BSA/OT)	20.1 ± 1.6	19.6 ± 1.9	20.1 ± 1.5
(AuNP/OT)/BSA	19.1 ± 2.2	20.1 ± 2.1	19.7 ± 2.3

[a]DLS particle size of the as-synthesized AuNPs is 13.6 ± 1.3. DLS measurements were conducted ∼5 min after sample preparation. The two components in the parentheses in the three-component mixtures were mixed first and shaken for ∼5 min before the addition of the third component.

the OTs that do not induce significant AuNP aggregation within the first hour of OT and AuNP mixing. First, the particle size of the as-synthesized AuNPs is statistically identical to that of the OT adsorbed AuNPs. This result is expected because of the limited precision of the DLS method and relatively small size of the OT molecules. Second, the particle size of AuNP/BSA is about ∼6 nm larger than that of the as-synthesized AuNP diameter; this result is consistent with reports in the literature showing that the BSA-coated layer on AuNP is about ∼3 nm thick.[9] Third, AuNPs in all the AuNP/BSA/OT mixtures have essentially the same AuNP sizes as in AuNP/BSA, regardless of the OT structures tested and the sequence of the samples preparation. The fact that (AuNP/Cys)/BSA and (AuNP/GSH)/BSA have the same measured particle size as AuNP/BSA is particularly noteworthy. It strongly indicates that secondary BSA adsorption onto OT-covered AuNP is possible even when the OTs are hydrophilic. This experimental result is consistent with the literature reports that BSA can be adsorbed onto quartz plates and poly(ethylene glycol) (PEG)-functionalized planar gold surfaces.[33] The DLS data in Table 1 strongly suggest that secondary BSA adsorption occurred in all the sequential OT and BSA interactions with AuNP even though direct DLS measurements of the BSA binding onto other OT-covered AuNP is not possible because of the OT-adsorption-induced AuNP aggregation. However, it is currently unclear why only MBI- and 2MP-induced AuNP aggregation can be stopped by the subsequent BSA addition into the AuNP/OT mixtures.

The ξ-potential measurements (ELS and PALS) were unsuccessful for the AuNP/BSA and AuNP/BSA/OT mixtures. We found that BSA-coated AuNPs can deposit on the electrode, which makes reliable measurement difficult. No appreciable ξ-potential was obtained with BSA alone at a 10 μM concentration, which is inconsistent with the report by Franzen et al., who demonstrated that there is no measurable ξ-potential for BSA with concentration up to 100 μM.[10]

Sequential BSA and OT Interactions with AuNPs (AuNP/BSA)/OT. The sequential interactions of BSA and OT with AuNPs were recently studied using MBI and aminoacid thiols as example OTs.[13] All the OTs tested were adsorbed onto to BSA-coated AuNPs. However, only MBI was used in the aging experiments designed to study both OT adsorption kinetics and AuNP stability in (AuNP/BSA)/OT samples versus AuNP/BSA aging before MBI addition.[13] In that study, all AuNPs resisted aggregation regardless of whether the AuNP/BSA mixture was aged for 5 s or 2 days before MBI addition. This was attributed to the high binding affinity of BSA with AuNPs. It may also be due to the secondary BSA adsorption in the (AuNP/BSA)/MBI sample in light of the finding that BSA can adsorb onto AuNP by interacting with the MBI layer bound to the Au. Therefore, a better OT probe is needed to definitively answer whether or not the OT can displace BSA adsorbed onto AuNPs. In this work, TG was chosen as the molecular probe because significant secondary BSA adsorption onto a TG layer adsorbed to AuNPs has been excluded by studies with the AuNP/(BSA/TG) and (AuNP/TG)/BSA) samples. These data indicate that substantial AuNP aggregation should be observed in the (AuNP/BSA)/TG samples if substantial BSA displacement occurs. Figure 7

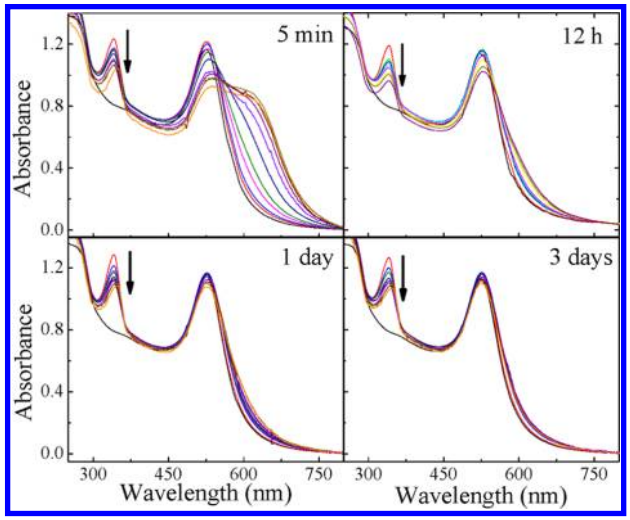

Figure 7. Representative time-resolved UV−vis spectra of (AuNP/BSA)/TG samples in which TG was added after aging AuNP/BSA mixtures for 5 min, 12 h, 1 day, and 3 days, respectively. The spectra shown each panel were taken at 7 s, 30 s, 1 min, 10 min, 2 h, 12 h, 1 day, and 3 days after the addition of TG. The (black) AuNP UV−vis spectrum is also shown in each plot. The concentrations of AuNP, BSA, and TG used in the analyses are 3.7 nM, 3.3 μM, and 16.6 μM, respectively.

showed the time-resolved UV−vis spectra obtained with a series of (AuNP/BSA)/TG samples in which TG was added after the AuNP/BSA mixtures had been aged for 5 min, 12 h, 1 day, and 3 days, respectively.

Several observations are noteworthy: First, TG adsorption onto the BSA-stabilized AuNPs is evident by the drop in TG's UV−vis absorbance with increasing (AuNP/BSA)/TG incubation time. This occurred regardless of the (AuNP/BSA) mixture's age. This quenching of the TG UV−vis absorption upon TG binding onto AuNPs is consistent with our recent observation with MBI.[13] Quenching is attributed to charge transfer between the surface adsorbate and AuNPs.[34,35] Second, (AuNP/BSA)/TG solution samples are mostly stable, even when (AuNP/BSA) is aged for only 5 min before the TG addition. This is in stark contrast to AuNP/TG, AuNP/(BSA/TG), and (AuNP/TG)/BSA systems, in which AuNPs completely aggregated and settled after overnight incubation (Figures 2 and 6). The longer AuNP/BSA is aged before the TG addition, the more stable the AuNPs in (AuNP/BSA)/TG

dx.doi.org/10.1021/jp310085u | J. Phys. Chem. C 2013, 117, 1366−1374

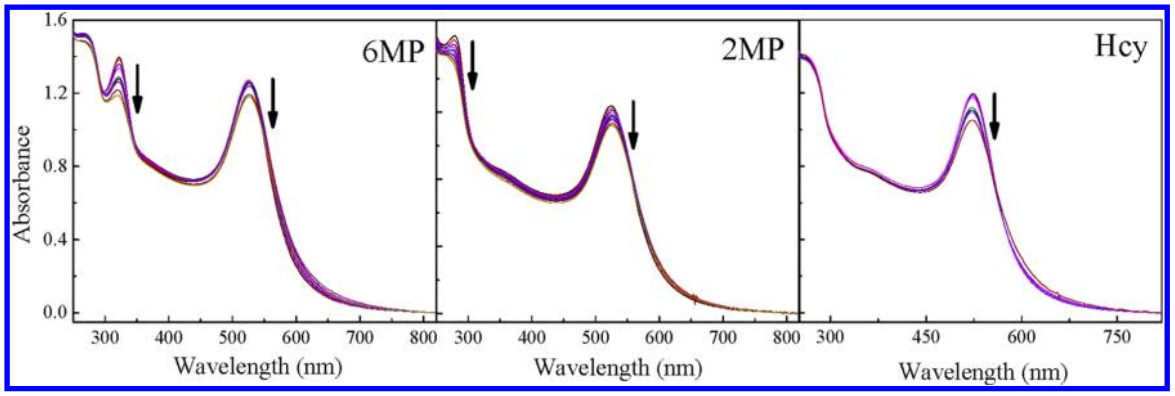

Figure 8. Representative time-resolved UV−vis spectra of (AuNP/BSA)/OT samples in which the OT was added after aging the AuNP/BSA mixture for 1 day. The spectra shown in (A−C) were taken at 7 s, 30 s, 1 min, 10 min, 2 h, 12 h, 1 day, and 3 days after the addition of the OT. The concentrations of AuNP, BSA, and OT used in all the analyses are 3.7 nM, 3.3 μM, and 16.6 μM, respectively.

samples become. This indicates that the BSA adlayer becomes increasingly stable on the AuNPs. This is consistent with our finding that a larger the fraction of AuNP surface is passivated by BSA against MBI adsorption as the AuNP/BSA aging period is increased.[13] Aging AuNP/BSA solutions before the addition of other OTs can also prevent AuNP aggregation (Figure 8). The time-dependent OT adsorption onto AuNPs in (AuNP/BSA)/2MP and (AuNP/BSA)/6MP samples was demonstrated by both the decreasing 2MP or 6MP UV−vis absorbance and the decreased AuNP LSPR absorbance in the 520 nm region. However, the Hcy adsorption onto AuNPs can only be deduced by the decreased AuNP LSPR absorbance because Hcy does not absorb in the UV−vis spectral region we explored.

The drastically enhanced stability against aggregation exhibited by (AuNP/BSA)/OT samples in comparison to that of corresponding AuNP/OT samples strongly suggests that BSA is the dominant ligand determining AuNP aggregation characteristics in (AuNP/BSA)/OT samples. This result is important since it excluded the possibility of substantial secondary OT adsorption in (AuNP/BSA)/OT samples. In other words, the subsequent OT adsorption onto AuNPs in the (AuNP/BSA)/OT samples resulted from the direct AuNP/OT interactions.

CONCLUSIONS

This work represents the first systematic study comparing simultaneous and sequential protein and OT interactions with AuNPs. The inclusion of a relatively large number of model OTs in this study enabled the exploration of how OT structure affects the AuNP stability against aggregation induced by OT adsorption in AuNP/OT, AuNP/(BSA/OT), (AuNP/OT)/BSA, and (AuNP/BSA)/OT samples. Among AuNP/BSA/OT mixtures with the same composition, AuNPs were most stable in (AuNP/BSA)/OT samples where BSA was added to the AuNP first, followed by subsequent OT addition. The simultaneously mixed AuNP/(BSA/OT) samples followed in stability. Finally, sequentially mixed (AuNP/OT)/BSA samples, where the OT was added before BSA into colloidal AuNP solutions, were least stable. Since the AuNP/BSA/OT mixtures have the exact the same composition and differ only in the sequence how the different components are mixed, the dependence of the AuNP aggregation on the ligand addition sequence in the AuNP/BSA/OT mixtures indicates that competitive BSA and OT binding onto AuNPs is kinetically controlled. Otherwise, one would expect the same AuNP stability in the AuNP/BSA/OT mixtures regardless of the addition sequence of the individual components.

The fact that aging (AuNP/BSA) before OT addition increases the AuNP stability on one hand provides an effective method for fabricating stable BSA and OT coadsorbed AuNPs. On the other hand, it indicates that the protein/AuNP binding affinity is strongly age-dependent. This casts doubt on the usefulness and reliability of the BSA binding constants with AuNPs. Our present and recent studies suggest that it is unlikely that BSA reaches an equilibrium state on AuNPs within a reasonable experimental time frame in which protein remains intact on the AuNPs (2 days, for example). This time-dependent BSA binding affinity with AuNPs may explain the vastly different (from 10^5 to 10^{11} M^{-1}) BSA "equilibrium binding constants" with AuNPs reported by various groups.[5−8] Besides providing new insights into our fundamental understanding of multicomponent protein/OT interactions with AuNPs, this work may provide guidance for fabricating biocompatible protein and organothiol coadsorbed AuNPs that can be envisioned for a series of biomedical applications including biosensing and drug delivery.

ASSOCIATED CONTENT

Supporting Information

Organothiols interactions with AuNPs. This material is available free of charge via the Internet at http://pubs.acs.org.

AUTHOR INFORMATION

Corresponding Author

*E-mail dz33@msstate.edu.

Notes

The authors declare no competing financial interest.

ACKNOWLEDGMENTS

This work was supported in part by a NSF Grant (EPS-0903787) and a NSF CAREER Award (CHE 1151057) provided to D.Z. The TEM work was carried out at Florida State University, and the TEM facility at FSU is funded and supported by the Florida State University Research Foundation, National High Magnetic Field Laboratory (NSF-DMR-0654118) and the State of Florida.

REFERENCES

(1) Saha, K.; Agasti, S. S.; Kim, C.; Li, X.; Rotello, V. M. *Chem. Rev.* **2012**, *112*, 2739−2779.
(2) Dykman, L.; Khlebtsov, N. *Chem. Soc. Rev.* **2012**, *41*, 2256−2282.
(3) Love, J. C.; Estroff, L. A.; Kriebel, J. K.; Nuzzo, R. G.; Whitesides, G. M. *Chem. Rev.* **2005**, *105*, 1103−1170.
(4) Lacerda, S. H. D. P.; Park, J. J.; Meuse, C.; Pristinski, D.; Becker, M. L.; Karim, A.; Douglas, J. F. *ACS Nano* **2009**, *4*, 365−379.
(5) Li, N.; Zeng, S.; He, L.; Zhong, W. *Anal. Chem.* **2010**, *82*, 7460−7466.
(6) Tsai, D.-H.; DelRio, F. W.; Keene, A. M.; Tyner, K. M.; MacCuspie, R. I.; Cho, T. J.; Zachariah, M. R.; Hackley, V. A. *Langmuir* **2011**, *27*, 2464−2477.
(7) Wangoo, N.; Suri, C. R.; Shekhawat, G. *Appl. Phys. Lett.* **2008**, *92*, 133104.
(8) Treuel, L.; Malissek, M.; Gebauer, J. S.; Zellner, R. *ChemPhysChem* **2010**, *11*, 3093−3099.
(9) Casals, E.; Pfaller, T.; Duschl, A.; Oostingh, G. J.; Puntes, V. *ACS Nano* **2010**, *4*, 3623−3632.
(10) Brewer, S. H.; Glomm, W. R.; Johnson, M. C.; Knag, M. K.; Franzen, S. *Langmuir* **2005**, *21*, 9303−9307.
(11) Sen, T.; Mandal, S.; Haldar, S.; Chattopadhyay, K.; Patra, A. *J. Phys. Chem. C* **2011**, *115*, 24037−24044.
(12) Zhang, D.; Neumann, O.; Wang, H.; Yuwono, V. M.; Barhoumi, A.; Perham, M.; Hartgerink, J. D.; Wittung-Stafshede, P.; Halas, N. J. *Nano Lett.* **2009**, *9*, 666−671.
(13) Vangala, K.; Ameer, F.; Salomon, G.; Le, V.; Lewis, E.; Yu, L.; Liu, D.; Zhang, D. *J. Phys. Chem. C* **2012**, *116*, 3645−3652.
(14) Ionita, P.; Volkov, A.; Jeschke, G.; Chechik, V. *Anal. Chem.* **2007**, *80*, 95−106.
(15) Schlenoff, J. B.; Li, M.; Ly, H. *J. Am. Chem. Soc.* **1995**, *117*, 12528−12536.
(16) Walczyk, D.; Bombelli, F. B.; Monopoli, M. P.; Lynch, I.; Dawson, K. A. *J. Am. Chem. Soc.* **2010**, *132*, 5761−5768.
(17) Haiss, W.; Thanh, N. T. K.; Aveyard, J.; Fernig, D. G. *Anal. Chem.* **2007**, *79*, 4215−4221.
(18) Zhang, D.; Xie, Y.; Mrozek, M. F.; Ortiz, C.; Davisson, V. J.; Ben-Amotz, D. *Anal. Chem.* **2003**, *75*, 5703−5709.
(19) Delfino, I.; Cannistraro, S. *Biophys. Chem.* **2009**, *139*, 1−7.
(20) Maiorano, G.; Sabella, S.; Sorce, B.; Brunetti, V.; Malvindi, M. A.; Cingolani, R.; Pompa, P. P. *ACS Nano* **2010**, *4*, 7481−7491.
(21) Xie, H.; Tkachenko, A. G.; Glomm, W. R.; Ryan, J. A.; Brennaman, M. K.; Papanikolas, J. M.; Franzen, S.; Feldheim, D. L. *Anal. Chem.* **2003**, *75*, 5797−5805.
(22) Tessier, P. M.; Jinkoji, J.; Cheng, Y.-C.; Prentice, J. L.; Lenhoff, A. M. *J. Am. Chem. Soc.* **2008**, *130*, 3106−3112.
(23) Ansar, S. M.; Haputhanthri, R.; Edmonds, B.; Liu, D.; Yu, L.; Sygula, A.; Zhang, D. *J. Phys. Chem. C* **2011**, *115*, 653−660.
(24) Lim, S. I.; Zhong, C.-J. *Acc. Chem. Res.* **2009**, *42*, 798−808.
(25) Bellino, M. G.; Calvo, E. J.; Gordillo, G. *Phys. Chem. Chem. Phys.* **2004**, *6*, 424−428.
(26) Patel, G.; Menon, S. *Chem. Commun.* **2009**, 3563−3565.
(27) Ansar, S. M.; Haputhanthri, R.; Edmonds, B.; Liu, D.; Yu, L.; Sygula, A.; Zhang, D. *J. Phys. Chem. C* **2010**, *115*, 653−660.
(28) Dasary, S. S. R.; Singh, A. K.; Senapati, D.; Yu, H.; Ray, P. C. *J. Am. Chem. Soc.* **2009**, *131*, 13806−13812.
(29) Lu, C.; Zu, Y. *Chem. Commun.* **2007**, 3871−3873.
(30) Rostkowska, H.; Lapinski, L.; Nowak, M. J. *J. Phys. Chem. A* **2003**, *107*, 804−809.
(31) Moulin, A. M.; O'Shea, S. J.; Badley, R. A.; Doyle, P.; Welland, M. E. *Langmuir* **1999**, *15*, 8776−8779.
(32) Silin, V.; Weetall, H.; Vanderah, D. J. *J. Colloid Interface Sci.* **1997**, *185*, 94−103.
(33) Ogi, H.; Fukunishi, Y.; Nagai, H.; Okamoto, K.; Hirao, M.; Nishiyama, M. *Biosens. Bioelectron.* **2009**, *24*, 3148−3152.
(34) Franzen, S.; Folmer, J. C. W.; Glomm, W. R.; O'Neal, R. *J. Phys. Chem. A* **2002**, *106*, 6533−6540.
(35) Reyes, E.; Madueno, R.; Blazquez, M.; Pineda, T. *J. Phys. Chem. C* **2010**, *114*, 15955−15962.